PET of Human Prostate Cancer Xenografts in Mice with Increased Uptake of $^{64}CuCl_2$

Fangyu Peng[1–3], Xin Lu[1], James Janisse[4], Otto Muzik[1,2], and Anthony F. Shields[3,5]

[1]Department of Pediatrics, School of Medicine, Wayne State University, Detroit, Michigan; [2]Department of Radiology, School of Medicine, Wayne State University, Detroit, Michigan; [3]Barbara Ann Karmanos Cancer Institute, School of Medicine, Wayne State University, Detroit, Michigan; [4]Center for Healthcare Effectiveness Research, School of Medicine, Wayne State University, Detroit, Michigan; and [5]Department of Medicine, School of Medicine, Wayne State University, Detroit, Michigan

Our objective was to determine whether human prostate cancer xenografts in mice can be localized by PET using $^{64}CuCl_2$ as a probe (^{64}Cu PET). **Methods:** Athymic mice bearing human prostate cancer xenografts were subjected to ^{64}Cu PET, followed by quantitative analysis of the tracer concentrations and immunohistochemistry study of human copper transporter 1 expression in the tumor tissues. **Results:** Human prostate cancer xenografts expressing high levels of human copper transporter 1 were well visualized on the PET images obtained 24 h after injection but not on the images obtained 1 h after injection. PET quantitative analysis demonstrated a high concentration of $^{64}CuCl_2$ in the tumors in comparison to that in the left shoulder regions (percentage injected dose per gram of tissue: 3.6 ± 1.3 and 0.6 ± 0.3, respectively; $P = 0.004$), at 24 h after injection. **Conclusion:** The data from this study suggested that locally recurrent prostate cancer might be localized with ^{64}Cu PET using $^{64}CuCl_2$ as a probe.

Key Words: prostate cancer; positron emission tomography; human copper transporter 1; copper (II)-64 chlorides

J Nucl Med 2006; 47:1649–1652

Prostate cancer is the second leading cause of death in men (*1*). ^{18}F-FDG PET has been widely used for localization and staging of many cancers, but its utility for detection of the local recurrence of prostate cancer is limited by excretory ^{18}F-FDG activity in the urinary bladder (*2–4*). Multiple tracers have been investigated for imaging locally recurrent prostate cancer, such as ^{11}C-acetate (*5*), ^{11}C-choline (*6,7*), and recently ^{18}F-FDG-1-(2-deoxy-2-fluoro-b-arabinofuranosyl)thymine (*8*). These new probes under investigation have their own strengths but also some limitations. It is worthwhile to search for additional new probes that may be used when the utility of the probes currently available is limited.

Copper is an essential nutrient in mammals, and copper homeostasis is delicately maintained by a network of copper transporters, chaperones, and efflux pumps (*9*). Human copper transporter 1 (hCtr1) is a high-affinity copper transporter that mediates cellular uptake of copper in humans and is highly expressed in the liver. After cloning of the hCtr1 gene (*10*), the mouse copper transporter 1 gene was cloned and showed an expression profile similar to that of hCtr1 (*11*). Recently, it was reported that extrahepatic mouse hepatoma grafts expressing high levels of mouse copper transporter 1 could be detected by ^{64}Cu PET using $^{64}CuCl_2$ as a probe (*12*). On the ^{64}Cu PET images, there was little background activity in the urinary bladder region because $^{64}CuCl_2$ was cleared mainly by the hepatobiliary pathway instead of renally. In view of the fact that human tumor tissues contain high concentrations of copper (*13,14*), we hypothesized that human prostate cancers express high levels of hCtr1 and can be detected by ^{64}Cu PET. To test this hypothesis, preliminary experiments were performed to determine whether human prostate cancer xenografts in mice can be localized with ^{64}Cu PET.

MATERIALS AND METHODS

Cells, Animals, and Human Prostate Cancer Xenografts in Mice

Human prostate cancer cells, PC-3 (ATCC), were cultured in RPMI 1640 medium supplemented with 10% fetal bovine serum, penicillin (100 U/mL), and streptomycin (100 mg/mL; BioSource International). Athymic mice (male; 4–5 wk old; body weight, 21.5–25.0 g) from Harlan Laboratory were used for this study, which was approved by the Animal Investigation Committee of Wayne State University. PC-3 cells (5×10^6/injection site) were injected subcutaneously in the right flank of the mice, and the tumor-bearing mice were subjected to PET studies when the tumor xenografts reached about 0.8 × 0.8 cm.

PET

The athymic mice bearing human prostate cancer xenografts were subjected to a PET study using a microPET R4 tomograph (Concorde Microsystems), in a protocol modified from that described previously (*12*). Briefly, the tumor-bearing mice were anesthetized with a mixture of ketamine (100 mg/kg) and xylazine (7 mg/kg) and positioned in spread-supine position on the PET bed. Initially, a 17-min transmission scan was acquired to correct for attenuation of the 511-keV photons. After the transmission

Received Mar. 31, 2006; revision accepted Jul. 6, 2006.

For correspondence or reprints contact: Fangyu Peng, MD, PhD, PET Center, Children's Hospital of Michigan, School of Medicine, Wayne State University, 3901 Beaubien Blvd., Detroit, MI 48201.

E-mail: fpeng@pet.wayne.edu

scan, the mice received an injection of $^{64}CuCl_2$ (74 kBq [2 μCi]/g of body weight) via the tail vein. At 1 and 24 h after injection of the tracer, whole-body data acquisition consisting of 2 overlapping frames of 15-min duration (2-cm overlap) was started. The ^{64}Cu radionuclide (half-life, 12.7 h; decay characteristics, 19% β^+ and 40% β^-) was produced in a cyclotron with a radionuclide purity of more than 99% and was supplied as $^{64}CuCl_2$ in an HCl solution (0.1 mol/L) by the Mallinckrodt Institute of Radiology, Washington University. The whole-body images were corrected for attenuation using the previously acquired transmission scans and reconstructed using an iterative ordered-subsets expectation maximization 2-dimensional algorithm (*15*). PET images were visually assessed for biodistribution of the tracer and localization of the tumor xenografts.

PET Quantitative Analysis of Tracer Concentration

For maximum sensitivity, the PET data were reconstructed using measured attenuation, scatter correction, and the ordered-subsets expectation maximization 2-dimensional iterative algorithm, yielding an isotropic spatial resolution of about 2 mm in full width at half maximum. The images were subsequently processed using ASIPro PET data analysis software (Concorde Microsystems). A calibration factor predetermined by scanning a phantom was used to convert counts/pixel/min to kBq (μCi)/cm^3 for the tracer ^{64}Cu. Regions of interest were drawn in all planes over the tumor, liver, and soft-tissue region on the left flank opposite the tumor. The average tracer concentration (kBq [μCi]/cm^3) for each defined area was obtained as a weighted (by area) average of the tracer concentration obtained from all image planes in which regions of interest for that particular tissue region were defined. Finally, the decay-corrected percentage of injected dose per gram of tissue (%ID/g) for each area was calculated by dividing the obtained average tracer concentration (kBq [μCi]/cm^3) in the region by the injected activity (kBq [μCi]) over mouse body weight (g).

Radioactivity Assay for Tissue Tracer Concentration

Upon completion of the PET studies at 1 and 24 h after injection, the tumor-bearing mice were euthanized under anesthesia and postmortem tissues were harvested, weighed, and counted for radioactivity with a Packard Cobra II γ-counter (Perkin-Elmer). Tissue radioactivity was calculated and expressed as a decay-corrected %ID/g.

Immunohistochemistry Study for Expression of hCtr1

For study of hCtr1 expression, postmortem tumor tissues were harvested, fixed in 10% buffered formalin, embedded in paraffin, and then sectioned into 5-μm sections for immunohistochemistry study. After incubation with an hCtr1-specific polyclonal antibody (Novus Biologicals) at a dilution of 1:250, the immunoreactivity against hCtr1 was visualized by reaction with horseradish peroxidase–labeled goat–antirabbit secondary antibody (Vector Laboratories). Microscopic images of the stained sections were recorded with an Olympus microscope equipped with a Spot digital camera (Diagnostic Instruments). Tissue sections incubated with normal rabbit serum were used as a negative control, whereas mouse liver tissue sections were included as a positive control.

Statistical Analysis

Data of quantitative PET analysis and radioactivity count ex vivo were expressed by a mean and SD. Repeated-measures ANOVA was performed to determine whether tracer uptake observed using PET (%ID/g) differed significantly from tracer uptake of $^{64}CuCl_2$ determined using a radioactivity assay ex vivo. A significant overall F value was followed by a limited number of post hoc tests comparing tumor tissue uptake with uptake in each of the other tissues. Because the number of post hoc comparisons for each outcome was less than the number of levels of the repeated factor, no correction for multiple comparisons was used. A P value of less than 0.05 was considered to represent statistical significance.

RESULTS

^{64}Cu PET of Human Prostate Cancer Xenografts in Mice

Ten athymic mice bearing human prostate cancer xenografts were imaged using PET at 1 h ($n = 5$) or 24 h ($n = 5$) after intravenous administration of $^{64}CuCl_2$, followed by postmortem tissue radioactivity assay. Human prostate cancer xenografts were well visualized on the PET images obtained at 24 h after injection (Fig. 1) but were only faintly seen on PET images obtained at 1 h after injection. Intense tracer activity was present in the liver, with little tracer activity observed in the urinary bladder region. PET quantitative analysis demonstrated increased uptake of $^{64}CuCl_2$ in the tumor (3.6 ± 1.3 %ID/g) at 24 h after injection. This activity was about 6-fold higher than that measured from the left shoulder region (0.6 ± 0.3 %ID/g). As expected, a high tracer uptake (17.5 ± 3.9 %ID/g) was determined in the liver. After a significant overall repeated-measures ANOVA ($F_{2,8} = 77.51$, $P < 0.001$), post hoc tests revealed that tracer uptake in tumor tissue was significantly higher than tracer uptake in the shoulder region ($F_{1,4} = 34.33$, $P = 0.004$) but lower than tracer uptake in the liver ($F_{1,4} = 58.14$, $P = 0.002$).

Distribution of $^{64}CuCl_2$ in Tumor-Bearing Mice by Radioactivity Assay Ex Vivo

The biodistribution of $^{64}CuCl_2$ in the tumor-bearing mice was further investigated through radioactivity assay of postmortem mouse tissues harvested on completion of the imaging studies at 1 h after injection ($n = 5$) and 24 h after

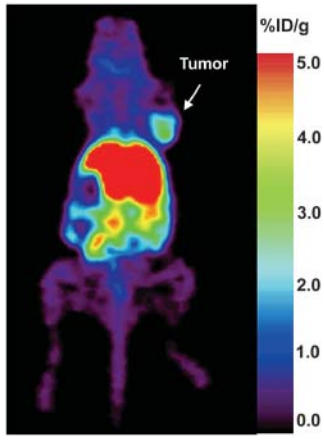

FIGURE 1. Human prostate cancer xenograft is well visualized on PET image obtained at 24 h after injection. Prominent tracer activity is seen in liver and intestinal tracts in abdomen (excreted activity from liver), with little tracer activity in region of urinary bladder. To allow contrast between organs with a relatively lower %ID/g than that of liver, we expanded color scale at bottom 25% of maximum. Color saturation is seen at location of liver, which has %ID/g of between 15% and 20%.

injection ($n = 5$) (Fig. 2). At 1 h after injection, the highest tracer uptake was found in the liver (24.7 ± 4.4 %ID/g), followed by the lungs (11.8 ± 3.6 %ID/g), kidneys (9.6 ± 4.4 %ID/g), heart (6.6 ± 1.4 %ID/g), tumor tissues (3.0 ± 0.7 %ID/g), spleen (2.2 ± 0.7 %ID/g), muscles (1.7 ± 1.5 %ID/g), blood (1.5 ± 0.4 %ID/g), and brain (0.3 ± 0.1 %ID/g). At 24 h after injection, tracer uptake in the tumor tissue increased to 4.4 ± 1.1 %ID/g and tracer uptake in the spleen slightly increased to 2.9 ± 1.5 %ID/g. In contrast, tracer uptake in all other tissues decreased (liver, 15.6 ± 3.1 %ID/g; lungs, 4.6 ± 0.7 %ID/g; kidneys, 7.9 ± 2.1 %ID/g; heart, 4.2 ± 1.5 %ID/g; muscles, 0.8 ± 0.3 %ID/g; blood, 0.8 ± 0.2 %ID/g; brain, 0.6 ± 0.2 %ID/g). Moreover, tissue uptake values measured by ex vivo radioactivity assay (tumor, liver, left shoulder soft tissue) were slightly higher than those determined using PET quantitative analysis. This discrepancy may be related to small variations of tracer concentration in different regions of the organs.

The tracer uptake values obtained from various tissues at 24 h after injection were initially tested using an overall repeated-measures ANOVA, which was found to be significant ($F_{8,32} = 56.64$, $P < 0.001$). Post hoc tests revealed that tracer uptake in the tumor tissue was significantly higher than that in the shoulder region ($P = 0.003$), brain ($P = 0.001$), and blood ($P = 0.001$) but lower than that in the liver ($P = 0.001$) and kidneys ($P = 0.018$). No significant differences in tracer uptake were found between the tumor tissue and the lungs ($P = 0.80$), spleen ($P = 0.22$), or heart ($P = 0.86$). Moreover, the overall repeated-measures ANOVA at 1 h after injection was also significant ($F_{8,32} = 67.30$, $P < 0.001$). Post hoc tests revealed that tracer uptake in the tumor tissue was significantly higher than that in the shoulder region ($P = 0.023$), brain ($P = 0.001$), and blood ($P = 0.012$) but lower than that in the liver ($P < 0.001$), kidney ($P = 0.019$), lung ($P = 0.003$), and heart ($P = 0.007$). Differences between the tumor tissue and the spleen ($P = 0.10$) were not significant. Finally, to determine whether the tracer uptake pattern observed in organs differed between 1 and 24 h after injection, we applied a mixed-design repeated-measures ANOVA with the organs as the within-subjects factor and the 2 time points as the between-subjects factor. We found a highly significant difference ($P < 0.001$) between the tracer uptake pattern observed at 1 h after injection and that observed at 24 h.

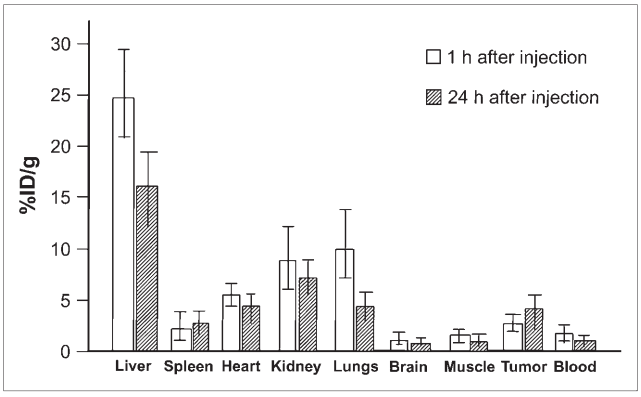

FIGURE 2. Distribution of $^{64}CuCl_2$ as determined by radioactivity assay in athymic mice bearing human prostate cancer xenografts. Postmortem tissues were harvested at 1 h ($n = 5$) or 24 h ($n = 5$) after intravenous injection of tracer. In comparison to tracer concentrations obtained at 1 h after injection, tracer concentrations obtained at 24 h after injection were higher in tumor and spleen tissues but lower in other tissues.

HCtr1 Is Highly Expressed in Human Prostate Cancer Xenografts Implanted in Mice

Strong hCtr1 immunoreactivity was seen on tumor tissue sections incubated with the hCtr1-specific antibody (Fig. 3A) but not on tissue sections incubated with normal rabbit serum (Fig. 3B). As expected, hCtr1 immunoreactivity observed on prostate cancer xenograft tissue was less intense than that seen on tissue sections of mouse liver but more intense than that seen on tissue sections of mouse muscle.

DISCUSSION

The successful detection of human prostate cancer xenografts in mice by ^{64}Cu PET (Fig. 2) suggests that ^{64}Cu PET may be useful in several applications: for detection of local recurrence in patients presenting with rising blood levels of prostate-specific antigen after radiation therapy of primary prostate cancer but in whom conventional imaging studies have failed to localize a viable tumor in the prostate bed; for detection of primary prostate cancer if a higher concentration of $^{64}CuCl_2$ has accumulated in cancerous tissues than in normal tissues or in tissues of a benign disorder such as hyperplasia; and for detection of other genitourinary cancers, such as bladder cancer, if increased uptake of $^{64}CuCl_2$ is also present in these tumors. The fact that human prostate xenografts were visualized on the images obtained at 24 h after injection but not on the images obtained at 1 h after injection differs from the behavior of the mouse hepatoma xenografts reported previously (*12*). This difference may be explained by the lower

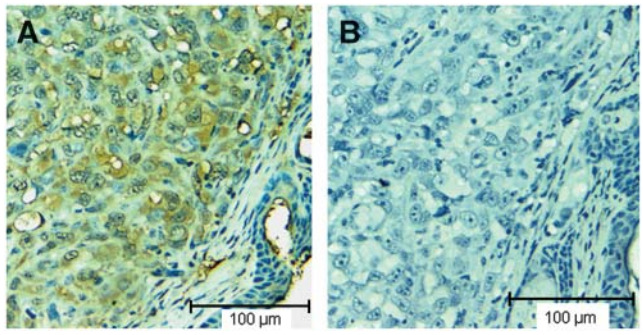

FIGURE 3. Strong hCtr1 immunoreactivity is seen on this section of human prostate cancer xenograft tissues after incubation with polyclonal antibody specific for hCtr1 (brown horseradish peroxidase product) (A) but was not seen on tissue sections of negative control. (B) Tissue sections were counterstained with DAPI (blue) to show cell nuclei.

expression of hCtr1 in prostate cancer relative to hepatoma and the prolonged time required for accumulation of the tracer, regulated by a balance of the tracer uptake by hCtr1 and washout by copper efflux pumps such as ATP7A and ATP7B. In a clinical setting, the patients may be subjected to ^{18}F-FDG PET for metastasis on the first day, followed by injection with $^{64}CuCl_2$ for emission scanning on the next day to localize the tumor lesions in the prostate bed.

Like other imaging technologies under investigation, ^{64}Cu PET has some limitations. It is limited in the detection of hepatic metastases of prostate cancer because of the high background $^{64}CuCl_2$ activity mediated by endogenous hCtr1. Its sensitivity and specificity for the detection of abdominal metastasis may be lowered by excretory $^{64}CuCl_2$ activity in the intestinal tracts. Another concern is potential side effects associated with the radiocytotoxicity of $^{64}CuCl_2$, an attribute useful for radionuclide cancer therapy (*16,17*). A tracer dose of radioactive $^{64}CuCl_2$ (185–370 MBq [5–10 mCi]) was previously used for scintiscans of whole-body radioactive copper distribution in patients with Wilson's disease (*18,19*) and was not associated with significant side effects or toxicity to normal organs. A dosimetry study is necessary to determine a safe tracer dose of $^{64}CuCl_2$ for PET of prostate cancer.

Because hCtr1 plays a major role in the cellular uptake of copper in humans (*9,10*), expression of hCtr1 in human prostate cancer xenografts was investigated by an immunohistochemistry study with an hCtr1-specific antibody. As expected, high levels of hCtr1 immunoreactivity were found in the tumor tissues (Fig. 3). Additional studies are needed to prove that increased uptake of $^{64}CuCl_2$ in prostate cancer tissues was mediated by hCtr1 overexpressed in those tissues. It will also be interesting to study the expression of hCtr1 in various tumors and the quantitative relationship of hCtr1 expression and uptake of the tracer, $^{64}CuCl_2$, by various tumors. If overexpression of hCtr1 is indeed found to be responsible for increased uptake of $^{64}CuCl_2$ by human prostate cancer, ^{64}Cu PET may provide additional information for clinical management of prostate cancer: The hCtr1 expression level may be related to the aggressiveness or prognosis of the prostate cancer, and hCtr1 expression may be related to the response of prostate cancer to cisplatin chemotherapy because hCtr1 was recently reported to be able to mediate cellular uptake of cisplatin (*20*).

CONCLUSION

The data from this study suggested that locally recurrent prostate cancer might be localized with ^{64}Cu PET using $^{64}CuCl_2$ as a probe.

ACKNOWLEDGMENTS

The authors thank Jianguo Liu for assistance with the immunohistochemistry study of hCtr1. This project was partly funded by a faculty research development grant awarded by the Departments of Pediatrics and Radiology, School of Medicine, Wayne State University. The production of ^{64}Cu at Washington University School of Medicine is supported by NCI grant R24 CA86307.

REFERENCES

1. Weir HK, Thun MJ, Hankey BF, et al. Annual report to the nation on the status of cancer, 1975-2000, featuring the uses of surveillance data for cancer prevention and control. *J Natl Cancer Inst.* 2003;95:1276–1299.
2. Effert PJ, Bares R, Handt S, Wolff JM, Bull U, Jakse G. Metabolic imaging of untreated prostate cancer by positron emission tomography with ^{18}fluorine-labeled deoxyglucose. *J Urol.* 1996;155:994–998.
3. Schöder H, Larson SM. Positron emission tomography for prostate, bladder, and renal cancer. *Semin Nucl Med.* 2004;34:274–292.
4. Jana S, Blaufox MD. Nuclear medicine studies of the prostate, testes, and bladder. *Semin Nucl Med.* 2006;36:51–72.
5. Kotzerke J, Volkmer BG, Neumaier B, Gschwend JE, Hautmann RE, Reske SN. Carbon-11 acetate positron emission tomography can detect local recurrence of prostate cancer. *Eur J Nucl Med Mol Imaging.* 2002;29:1380–1384.
6. Hara T, Kosaka N, Kishi H. PET imaging of prostate cancer using carbon-11-choline. *J Nucl Med.* 1998;39:990–995.
7. Kwee SA, Wei H, Sesterhenn I, Yun D, Coel MN. Localization of primary prostate cancer with dual-phase ^{18}F-fluorocholine PET. *J Nucl Med.* 2006;47: 262–269.
8. Sun H, Sloan A, Mangner TJ, et al. Imaging DNA synthesis with [^{18}F]FMAU and positron emission tomography in patients with cancer. *Eur J Nucl Med Mol Imaging.* 2005;32:15–22.
9. Puig S, Thiele DJ. Molecular mechanisms of copper uptake and distribution. *Curr Opin Chem Biol.* 2002;6:171–180.
10. Zhou B, Gitschier J. hCTR1: a human gene for copper uptake identified by complementation in yeast. *Proc Natl Acad Sci U S A.* 1997;94:7481–7486.
11. Lee J, Prohaska JR, Dagenais SL, Glover TW, Thiele DJ. Isolation of a murine copper transporter gene, tissue specific expression and functional complementation of a yeast copper transport mutant. *Gene.* 2000;254:87–96.
12. Peng F, Liu J, Wu J, Lu X, Muzik O. Mouse extra-hepatic hepatoma detected on microPET using copper (II)-64 chloride uptake mediated by endogenous mouse copper transporter 1. *Mol Imaging Biol.* 2005;7:325–329.
13. Diez M, Arroyo M, Cerdan FJ, Munoz M, Martin MA, Balibrea JL. Serum and tissue trace metal levels in lung cancer. *Oncology.* 1989;46:230–234.
14. Gupta SK, Shukla VK, Vaidya MP, Roy SK, Gupta S. Serum and tissue trace elements in colorectal cancer. *J Surg Oncol.* 1993;52:172–175.
15. Hudson HM, Larkin RS. Accelerated image reconstruction using ordered subsets of projection data. *IEEE Trans Med Imaging.* 1994;13:601–609.
16. Apelgot S, Coppey J, Gaudemers A, et al. Similar lethal effect in mammalian cells for two radioisotopes of copper with different decay schemes, ^{64}Cu, ^{67}Cu. *Int J Radiat Biol.* 1989;55:365–384.
17. Connett JM, Anderson CJ, Guo LW, et al. Radioimmunotherapy with a ^{64}Cu-labeled monoclonal antibody: a comparison with ^{67}Cu. *Proc Natl Acad Sci U S A.* 1996;93:6814–6818.
18. Osborn SB, Szaz KF, Walshe JM. Studies with radioactive copper (^{64}Cu and ^{67}Cu): abdominal scintiscans in patients with Wilson's disease. *Q J Med.* 1969;38:467–474.
19. Walshe JM, Potter G. The pattern of the whole body distribution of radioactive copper (^{67}Cu, ^{64}Cu) in Wilson's disease and various control groups. *Q J Med.* 1977;46:445–462.
20. Ishida S, Lee J, Thiele DJ, Herskowitz I. Uptake of the anticancer drug cisplatin mediated by the copper transporter Ctr1 in yeast and mammals. *Proc Natl Acad Sci U S A.* 2002;99:14298–14302.